DNA actively contributes to gene expression of paired transcription factors.

Rosa Maritato[1], Alessia Medugno[1], Emanuela D'Andretta[1], Giulia De Riso[2,3], Mariangela Lupo[4], Salvatore Botta[6], Elena Marrocco[4], Mario Renda[4], Martina Sofia[4], Maria Laura Bacci[5], and Enrico Maria Surace[1*]

[1]Department of Translational Medicine, University of Naples Federico II, Naples, Italy. Telethon Institute of Genetics and Medicine, Napoli, Italy.
[2]Department of Molecular Medicine and Medical Biotechnology, University of Naples Federico II, Naples, Italy
[3] AOU Federico II, Naples, Italy
[4] Telethon Institute of Genetics and Medicine (TIGEM), Pozzuoli, Italy
[5]Department of Veterinary Medical Sciences, University of Bologna, Bologna, Italy
[6]Department of Translational Medical Science, University of Campania Luigi Vanvitelli, Naples Italy

[*]Address correspondence to: Enrico Maria Surace, Department of Translational Medical Sciences (DiSMeT) University of Naples "Federico II", Italy, Via Pansini, 5 - 80131 – Napoli.
Email: enricomaria.surace@unina.it
ORCID: https://orcid.org/0000-000-2-29

DNA, by interacting with transcriptional regulators, determines gene expression, yet it is not known whether the DNA sequence itself actively contributes to gene expression. Here we show that changing the nucleotide sequence interposed between CRX and NRL binding sites (BS) of the *RHODOPSIN* (*RHO*) promoter led to uncorrelated gene expression variation. Mutual exchange of human and mouse homolog CRX-NRL-linking sequences, although divergent, conferred similar and species-specific gene expression levels. Interfering these DNA features with orthogonal proteins enables differential gene expression depending on the orientation linker sequence relative to the two BS. The results imply an active role of DNA itself in determining RHO expression levels.

DNA encodes gene expression by storing information on regulators of transcription, such as transcription factors (TFs), and providing them with specific short sequences (TF binding sites, TFBS) that they recognize and bind[1]. Thus, DNA sequence acts as a harbor for TFs docking by determining the order, orientation, and spacing of binding sites (syntax)[2]. Furthermore, multiple mutual recognition rules governing DNA-protein interactions have been established, including those underlying cooperative recognition by multiple TFs, and their impact on gene expression[3]. However, despite efforts, many aspects of the relationship between TFs and DNA sequence and gene expression remain unexplored. Here, we hypothesized that the DNA sequence interposed between a heterodimeric TF–TF (TF-DNA-TF complex) actively contributes to gene expression levels.

Previously, we showed that both a synthetic zinc finger protein (ZF-DB) with exclusive DNA-binding properties (without effector domains) and an ectopically expressed fully competent transcription factor (KLF15) block rhodopsin (Rho) expression when delivered to adult porcine retinal rod photoreceptors by Adeno-associated virus (AAV) vectors[4,5]. ZF-DB and KLF15 bind 20 and 9 nucleotides, partially overlapping (6 bp), of RHO proximal promoter region (-82 to -62 and -84 to -75 from the transcription start site, TSS, respectively; Fig.1a), suggesting that in terminally differentiated rods a very short DNA regulatory sequence contains key features controlling RHO expression.

Fig. 1. The DNA sequence interposed between CRX and NRL binding sites controls the expression levels of RHODOPSIN (RHO).a, Proximal promoter region of the human RHO (hRHOp) showing the coordinates of the locus, the BAT-1 and NRE elements (Ref), CRX and NRL TFs binding sites (in green and light blue, respectively) and the "footprints" onto hRHOp of the synthetic zinc finger protein (ZF-DB, on the negative strand, amaranth, below drawing of the six zinc-finger array of ZF-DB) and the TF KLF15(violet, on the positive strand, above drawing of the KLF15 including the effector domain in violet). **b**, Schematic representation of gene reporter assay with of Adeno-associated virus (AAV) vector carrying EGFP under the control of the RHO proximal promoter (pRHO) injected sub-retina in adult mice, on the right-handed panel immunofluorescence analysis on hRHOp 15 days post-injection. **c**, Sequences, and histogram (quantitative qPCR analysis measuring eGFP expression following AAV-eGFP in vivo retinal delivery in adult mice, methods), showing the impact of changing the syntax order, orientation, and spacing, of CRX and NRL BSs. **d,** Quantitative effects (qPCR) of CRX-NRL-link cloned in the 5' and 3' orientation (Prom-L). **e,** Nucleotides changes along CRX-NRL-link sequences in select mammalian species, sequences divergencies are highlighted. **f,** Quantitative effects (qPCR) of mutual changes of hRRU and mRRU insertion in murine and human RHO promoters, respectively. **g,** Quantitative effects (qPCR) of transfecting ZF-DB-5 or KLF15 in HEK-293 cell line onto hRHOp and Prom-L promoters, below the sequences bound by ZF-DB-5 and KLF15.

ZF-DB and KLF15 target a sequence between two extensively validated regulatory elements, BAT-1 and NRE [6], which are bound by the retinal-specific homeodomain transcription factor (TF), Cone Rod Homeobox protein (CRX)and by the rod photoreceptor-specific TF Neural Retina-specific Leucine zipper protein (NRL). CRX-NRL pairs operate synergistically to transactivate numerous rod-specific genes, including RHO[6].

On these bases, we assessed whether the 49 nucleotides long regulatory elements encompassing the CRX and NRL binding sites and the interposed linker sequence bound by ZF-DB and KLF15 may represent a regulatory unit (here named RHO regulatory unit, RRU) controlling RHO expression. To this end, we generated constructs for an in vivo AAV reporter assay, containing a human RHO proximal promoter fragment (hRHOp: -164bp from TSS and 95bp of 5'UTR-REF), to drive the expression of the enhanced Green Fluorescent Protein reporter gene (eGFP, Fig. 1b). Fifteen days after subretinal delivery of AAV-hRHOp-eGFP in adult mice, gene expression was confined to rod photoreceptors and resulted in robust gene expression (Fig. 1b). To dissect the contribution of DNA sequence determinants of RRU, we first mutated the CRX and NRL binding sites. AAV-hRHOp-eGFP carrying individual mutations in mCRX1, mCRX2 or NRL binding sites showed that each binding site is required to sustained eGFP reporter expression (Supplementary Fig. 1a). Next, we generated a duplication of the RRU (Prom-S), which almost doubled reporter expression levels, whereas deletion (Prom-R) resulted in negligible eGFP expression (Supplementary Fig. 1b). These results suggest that a 49 bp long RHO compact regulatory element containing CRX and NRL binding sites is necessary for RHO expression in adult mice.

To further dissect the DNA sequence determinants of the RRU, we changed the regulatory syntax, including CRX and NRL binding sites order, orientation, and the spacing between them. Mutual changes of CRX and NRL binding sites order (PromG-1), and concurrent change of order and orientation (PromG-2) resulted in less than half, and abolished reporter expression levels, respectively, relative to control (Fig. 1c). To manipulate the spacing between CRX and NRL binding sites, we generated three distinct non overlapping deletions of 5bp, Del-5', Del-C and Del-3', within CRX and NRL inter-sites. These deletions lead to a half DNA helical turn arrangement, thus placing CRX and NRL on opposite sides relative to native configuration. Reporter gene expression varied in these three constructs form basal (Del-3') to levels which outperform (Del-5') the native sequence (Fig. 1c). The fact that the same reduction of spacing resulted in highly differential eGFP expression levels implies that the source of the variation is contained into CRX and NRL linking sequence (from now on named CRX-NRL-link). This effect may be due to the generation of novel binding sites for either activators or repressors. To rule out this hypothesis we considered TFs in the human retina, and scanned each sequence for the respective BSs from the HOCOMOCO human collection (see Methods)[7]. NRL and CRX motifs were consistently located in the hRHOp-RRU, compatible with previously described occupancy on the human RHO promoter[8] and were also retained in all artificial promoter sequences here tested. Notably, we were not able to identify matches between TF expressed in the human retina and the CRX-NRL-link of both wild-type and artificial promoters (Supplementary Table S2).

Further we thought that a way to rule out the possibility to generate novel BSs was to maintain the length and nucleotide composition of the CRX-NRL-link but inverting the 5' and 3' orientation (Prom-L). This arrangement ensures a conservative configuration relative to the CRX-NRL-link, including its plus-minus DNA strands orientation. (Thus, the sole difference may affect the 5' and the 3' internal flanking sequence of CRX and NRL binding sites). The reporter expression levels in this arrangement were strongly reduced (Fig. 1d). This result indicates that the source of gene expression variation depends on the relative configuration of CRX, NRL BSs and the CRX-NRL-link.
To further characterize CRX-NRL-link, we mutated its sequence composition by generating both contiguous (7 to 10 nucleotides) and single nucleotide changes. These changes resulted in highly differential levels of reporter gene expression (Supplementary Fig. 1c), with no apparent correlation between the number of changes and the effect on reporter gene expression (Supplementary Fig. 1d). These results are consistent with those performed with a high-throughput method in the homologous sequence of the murine Rho promoter[9] and suggested that sequence composition of the linker is a key feature for RRU function .
Next, we compared the DNA sequence features of RRU along the mammalian phylogeny. The alignment of 100 mammalian genomes shows that, apart from rodents, the two CRX and the NRL binding sites are conserved (Fig. 1e; Supplementary Table S2). Another noteworthy feature is the conserved spacing of 22 nucleotides of the CRX-NRL-link. However, alternative nucleotide changes are present in several mammals, including the internal bases flanking core CRX and NRL binding sites (Fig. 1e). Therefore, given conserved spacing, nucleotide sequence varies across mammalian phylogeny.
Unlike other mammals, in rodents, and particularly in mouse and rat, RRU has one CRX binding site, and the CRX-NRL-link distance has one more nucleotide (23bp), while nucleotide sequence of the CRX-NRL-link diverges extensively (Fig. 1e). Thus, we compared the human and murine homolog sequence. To study murine RRU (mRRU), we generated AAV reporter constructs with the proximal murine rhodopsin promoter (mRHOp, 164 bp from the TSS and 78 bp from the 5'UTR). The murine promoter resulted in relatively lower reporter gene expression than the human counterpart (Fig. 1f). However, reciprocal replacement of human hRRU with mRRU in hRHOp and of mRRU with hRRU in mRHOp restored the species-specific reporter expression levels. This suggests that despite the divergences between the CRX-NRL-link, human and murine RRUs are functionally equivalent. Furthermore, between humans and mice, nucleotide divergence in the CRX-NRL-link corresponded to similar levels of reporter expression, unlike most constructs analyzed so far in humans, and as previously demonstrated in mice[9].

To determine whether these cis-regulatory sequence properties are retained, in isolation, in an unrelated trans-regulatory system in which retina-specific genes are not expressed, including CRX and NRL, we co-transfect HEK293 cell line with the same plasmids used to generate AAV vectors and those encoding for CRX and NRL (Methods). hRHOp-hRRU showed synergistic activation upon co-transfection with CRX and NRL and similar gene expression variation as observed in vivo on several constructs (Supplementary Fig. 1f). Next, we tested whether ZF-DB and KLF15 in vitro similarly engage the CRX-NRL-link sequence by repressing RHO promoter activity, as observed in vivo. Challenging hRHOp-hRRU WT resulted in significant repression of reporter expression (data not shown). To exclude intrusion into the NRL-binding site of the 6 ZF-DB fingers, we removed the first finger, obtaining ZF-DB-5 (Fig. 1g). This ZF-DB-5 mutant demonstrated similar RHO repression properties to those of ZF-DB in both RHO-P347S mice and WT pig retina in vivo (data not shown). Co-transfection of ZF-DB-5 or KLF15 with hRHOp-hRRU resulted in a reduction of reporter gene expression similar to that of ZF-DB (Fig. 1g). We then tested hRRU-Prom-L, which carries CRX-NRL-link sequence cloned in the 3'-5' direction, thus maintaining the binding sites for ZF-DB-5 and KLF15. Surprisingly, ZF-DB-5 and KLF15 promoted transactivation of RHO reporter expression (Fig. 1g). These results suggest that interfering CRX-NRL-link sequence with orthogonal proteins results in down- or up-regulation of gene expression, depending on the orientation of the sequence between CRX and NRL binding sites.

We have shown that fully differentiated rods require only a very short promoter sequence containing the binding sites of CRX and NRL to fully control RHO expression and that the expression levels of RHO are controlled by the nucleotide sequence linking them. Humans and mice show a species-specific sequence composition of CRX-NRL-link sequence to reach their RHO expression optimum. It has been suggested that RHO gene expression determines the size of the outer segment of the rod photoreceptors[10]; interestingly, this difference between mice and primates is compatible with that observed in this study[11].
We showed that the use of orthogonal DNA-binding proteins (ZF-DB and KLF15) induced complex effects on RHO expression, the underlying mechanism of which has yet to be determined. The ability of ZF-DB and KLF15 to block RHO expression in vivo at 20-fold lower concentrations than those of CRX and NRL[5,6] supports the possibility that the CRX-NRL-link is a DNA-free sequence, unbound from proteins. Consistently, this sequence was mapped as a DNase-unprotected region[12]. If these findings were also true for other TF pairs in the genome, the genetic space would become much larger than currently thought.

REFERENCES

1. Kim, S. & Wysocka, J. Deciphering the multi-scale, quantitative cis-regulatory code. *Mol. Cell* **83**, 373–392 (2023).
2. Farley, E. K., Olson, K. M., Zhang, W., Rokhsar, D. S. & Levine, M. S. Syntax compensates for poor binding sites to encode tissue specificity of developmental enhancers. *Proc. Natl. Acad. Sci.* **113**, 6508–6513 (2016).
3. Morgunova, E. & Taipale, J. Structural perspective of cooperative transcription factor binding. *Curr. Opin. Struct. Biol.* **47**, 1–8 (2017).
4. Botta, S. *et al.* Rhodopsin targeted transcriptional silencing by DNA-binding. *eLife* **5**, e12242 (2016).
5. Botta, S. *et al.* Targeting and silencing of rhodopsin by ectopic expression of the transcription factor KLF15. *JCI Insight* **2**, e96560 (2017).
6. Mitton, K. P. *et al.* The Leucine Zipper of NRL Interacts with the CRX Homeodomain. *J. Biol. Chem.* **275**, 29794–29799 (2000).
7. Kulakovskiy, I. V. *et al.* HOCOMOCO: towards a complete collection of transcription factor binding models for human and mouse via large-scale ChIP-Seq analysis. *Nucleic Acids Res.* **46**, D252–D259 (2018).
8. Cherry, T. J. *et al.* Mapping the *cis* -regulatory architecture of the human retina reveals noncoding genetic variation in disease. *Proc. Natl. Acad. Sci.* **117**, 9001–9012 (2020).
9. Kwasnieski, J. C., Mogno, I., Myers, C. A., Corbo, J. C. & Cohen, B. A. Complex effects of nucleotide variants in a mammalian *cis* -regulatory element. *Proc. Natl. Acad. Sci.* **109**, 19498–19503 (2012).

10. Price, B. A. *et al.* Rhodopsin Gene Expression Determines Rod Outer Segment Size and Rod Cell Resistance to a Dominant-Negative Neurodegeneration Mutant. *PLoS ONE* **7**, e49889 (2012).
11. Fu, Y. & Yau, K.-W. Phototransduction in mouse rods and cones. *Pflüg. Arch. - Eur. J. Physiol.* **454**, 805–819 (2007).
12. DesJardin, L. E. & Hauswirth, W. W. Developmentally important DNA elements within the bovine opsin upstream region. *Invest. Ophthalmol. Vis. Sci.* **37**, 154–165 (1996).

MATERIALS AND METHODS

Plasmid construction
The human rhodopsin proximal promoters (hRHOp, 164 bp from the transcription starting site (TSS) and 95bp of 5'UTR) and the mouse proximal promoter (mRHO, 164bp from the transcriptional starting site (TSS) and 78bp of 5'UTR) were generated by gene synthesis of Eurofins MWG® and cloned in pAAV2.1-eGFP using NheI and NotI restriction enzymes. All variant promoters of hRHOp (Prom-3A, Prom-H, Prom-Me, Del-3', Del-C, Prom-E, Prom-Q, Prom-N, Del-5', Prom-S, hRHOp-mRRU, mRHOp-hRRU, PromG-1, PromG-2, Prom-L, MutCRX1, MutCRX2, MutCRX1.2, MutNRL) were generated by gene synthesis of Eurofins MWG® and cloned in pAAV2.1-eGFP using NheI and NotI restriction enzymes. (Supplementary_TableS1)

AAV vector preparation and purification
AAV vectors were produced by by the TIGEM AAV Vector Core by triple transfection of HEK293 cells followed by two rounds of CsCl2 purification. For each viral preparation, physical titers [genome copies (GC)/mL] were determined by averaging the titer achieved by dot-blot analysis and by PCR quantification using TaqMan (Applied Biosystems, Carlsbad, CA, USA) (Doria et al., 2013).

Vector administration
All procedures were performed in accordance with institutional guidelines for animal research and all of the animal studies were approved by the authors. C57BL/6 mice (Charles Rivers Laboratories, Calco, Italy) were bred in the animal facility of the Biotechnology Centre of the Cardarelli Hospital (Naples, Italy).

Mice
Intraperitoneal injection of ketamine and medetomidine (100mg/kg and 0.25mg/kg respectively), then AAV vectors were delivered sub-retinal via a trans-scleral transchoroidal approach. (Botta 2016)
Each eye was co-injected with two AAV vectors: AAV vector carrying AAV-eGFP driven by human and murine proximal promoter variants (dose $1x10^9$GC/µl) and an AAV control vector encoding for human *RHO* gene driven by the GNAT1 proximal promoter (dose $1x10^8$GC/ µl) (Botta 2016). Mouse experimental groups were sized at n ≥ 4.

qReal Time PCR
RNAs from tissues were isolated using RNAeasy Mini Kit (Qiagen), according to the manufacturer protocol. cDNA was amplified from 1 µg isolated RNA using QuantiTect Reverse Transcription Kit (Qiagen), as indicated in the manufacturer instructions.
The PCRs with cDNA were carried out in a total volume of 20 µl, using 10 µl LightCycler 480 SYBR Green I Master Mix (Roche) and 400nM primers under the following conditions: pre-Incubation, 50°C for 5 min, cycling: 45 cycles of 95°C for 10 s, 60°C for 20 s and 72°C for 20 s. Each sample was analyzed in duplicate in two-independent experiments. Transcript levels of *eGFP* and h*RHO* were normalized against murine Gapdh and Actβ (DCt), and then the eGFP expression shown is obtained as fold change over control (co-injected vector). Furthermore, the AAV-hGNAT1-hRHO was co-injected to normalize the variability due to subretinal administration. We used the following primers: Act_forward (CAAGATCATTGCTCCTCCTGA) and Act_reverse (CATCGTACTCCTGCTTGCTGA), Gapdh_forward (GTCGGTGTGAACGGATTTG) and Gapdh_reverse (CAATGAAGGGGTCGTTGATG); eGFP_forward (ACGTAAACGGCCACAAGTTC) and eGFP_reverse (AAGTCGTGCTGCTTCATGTG); hRHO_forward (TCATGGTCCTAGGTGGCTTC) and hRHO_reverse (GGAAGTTGCTCATGGGCTTA).

Histological analysis
For morphological studies, after the mice were killed by cervical dislocation, the eyecups were harvested, fixed by immersion in 4% paraformaldehyde, and then embedded in OCT (KalteK). For each eye, 150 to 200 serial sections (10-µm thick) were cut along the horizontal plane; the sections were progressively distributed on 10 glass slides so that each slide contained 15 to 20 sections representative of the whole eye at different levels. Slides were coverslipped with Vectashield containing DAPI (4',6-diamidino-2-phenylindole; Vector laboratories, Burlingame, CA, USA) to stain cells nuclei and retinal histology was analyzed a Leica Fluorescence Microscope System (Leica Microsystems GmbH, Wetzlar, Germany).

Transient transfection and analysis of promoter activity by qReal Time PCR
HEK293 cells were plated in six-well plates at a density of $1x10^6$ cells/well in Dulbecco's modified Eagle's medium supplemented with 10% fetal bovine serum and 1% penicillin/streptomycin and grown for 24h a 37° C. The cells were transfected at 80% confluency using a TransIT-X2 Dynamic Delivery System (MIRUS), as indicated in the manufacturer instructions. We co-transfected the following constructs: 50 ng reported plasmid, 250ng of a plasmid encoding for human CRX, 125 ng of a plasmid expressing human NRL and 125ng CMV-ZF5 or CMV-KLF15 plasmid. The DNA amount was kept at 550 ng/well with pUC19. Cells were grown and harvested 48h post transfection in TRIzol™ Reagent (Life Technologies). The cDNA was amplified from 1 µg isolated RNA using QuantiTect Reverse Transcription Kit (Qiagen), as indicated in the manufacturer instructions. The PCRs with cDNA were carried out in a total volume of 20 µl, using 10 µl LightCycler 480 SYBR Green I Master Mix (Roche), 400nM primers under the following conditions: pre-Incubation, 50°C for 5 min, cycling: 45 cycles of 95°C for 10 s, 60°C for 20 s and 72°C for 20 s. Each sample was analysed in triplicate. Transcript levels of cells were measured by real-time PCR using the LightCycler 480 (Roche) and the following primers: PCR eGFP_forward (ACGTAAACGGCCACAAGTTC) and eGFP_reverse (AAGTCGTGCTGCTTCATGTG), GAPDH_forward (GAAGGTGAAGGTCGGAGT) and GAPDH_reverse (GAAGATGGTGATGGGATTTC). The eGFP expression shown is obtained normalizing to GAPDH.

Statistical analyses. Data are presented as mean ± Error bars indicate standard error mean (SEM). Statistical significance was computed using the One-Way Anova test (p-values ≤ 0.05), and post-hoc Dunnett's multiple comparisons test (p-values ≤ 0.05). Only in figure d we performed t-student test (p-values ≤ 0.0001).

Motif Scan
TF human motifs were retrieved from HOCOMOCO (version 11) (KulaKovskiy IV, 2018) and scanned on target sequences using FIMO (meme-suite 5.5) (Grant CE,2011), with background model derived from target sequence composition and parameters --norc and –thresh 0.01.
Matches with positive scores and p-value<0.01 were considered. Alternative matches for a given TF on the same sequence were disambiguated by considering the match with the highest score.

TF expression in retina
Transcript and protein expression data were retrieved from the Human Protein Atlas version 23.0 (https://www.proteinatlas.org/). We considered as positively expressed transcripts with normalized TPM >1 in human retina (n=13.114), and proteins with positive detection in photoreceptor cells (n=79).

Author contributions
EMS, conceived the study. RM, MP, SB, EMS, designed the experiments and analyzed data. MS, EM, performed histological analysis. GD performed bioinformatic analysis, EM, EMS, performed subretinal injection in mice. RM, EMS draft the manuscript. MLB supervised the in vivo studies in large animals. RM, AM, ED, GD, MP, SB, EM, MR, performed the molecular biology experiments. EMS wrote the manuscript and supervised the study.

Acknowledgments
This work was supported by the European Research Council/ERC grant 311682 “Allelechoker” (to EMS); ERC proof-of concept (ERC-POC). “Insight” 813223 (to EMS); Missione 4 - Center for Gene Therapy and Drugs based on RNA Technology- WP3.5- Stroke and other brain diseases, WP 3.5.7 (to EMS); Prin MUR: 2022LBZSTR (to EMS). We thank Fondazione Telethon and the TIGEM (Telethon Institute of Genetics and Medicine); the TIGEM Vector Core for vector production.

Competing interests
E.M.S., S.B. and E.M. are inventors on patents, “Artificial dna-binding proteins and uses thereof”, WO2015075154A3, US20160289284A1. E.M.S., S.B. and E.M. are inventors on a pending patent “Ectopically expressed transcription factors and uses thereof”, PCT/EP2018/086782, Department of Translational Medical Sciences (DiSMeT)University of Naples "Federico II", Italy, which may encompass the findings. The remaining authors declare no competing interests.

Figure 1

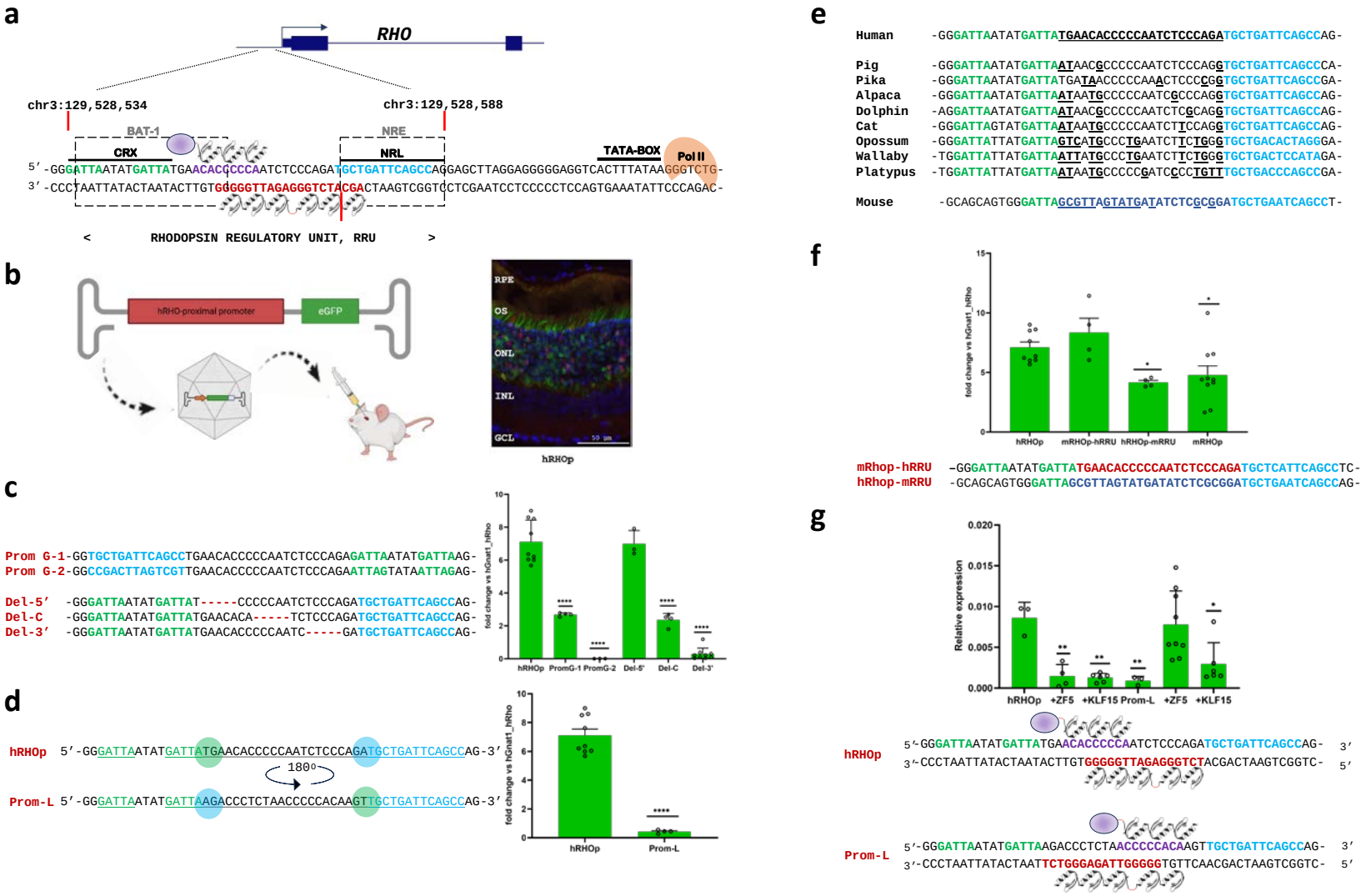
a
RHO
chr3:129,528,534
chr3:129,528,588
BAT-1
NRE
CRX
NRL
TATA-BOX
Pol II
5′-GGGATTAATATGATTATGAACACCCCAATCTCCCAGATGCTGATTCAGCCAGGAGCTTAGGAGGGGGAGGTCACTTTATAAGGGTCTG-
3′-CCCTAATTATACTAATACTTGTGGGGGTTAGAGGGTCTACGACTAAGTCGGTCCTCGAATCCTCCCCCTCCAGTGAAATATTCCCAGAC-
< RHODOPSIN REGULATORY UNIT, RRU >
b
hRHO-proximal promoter
eGFP
RPE
OS
ONL
INL
GCL
50 um
hRHOp
c
Prom G-1-GGTGCTGATTCAGCCTGAACACCCCCAATCTCCCAGAGATTAATATGATTAAG-
Prom G-2-GGCCGACTTAGTCGTTGAACACCCCCAATCTCCCAGAATTAGTATAATTAGAG-
Del-5′ -GGGATTAATATGATTAT-----CCCCCAATCTCCCAGATGCTGATTCAGCCAG-
Del-C -GGGATTAATATGATTATGAACACA-----TCTCCCAGATGCTGATTCAGCCAG-
Del-3′ -GGGATTAATATGATTATGAACACCCCCAATC-----GATGCTGATTCAGCCAG-
fold change vs hGnat1_hRho
hRHOp
PromG-1
PromG-2
Del-5′
Del-C
Del-3′
d
hRHOp 5′-GGGATTAATATGATTATGAACACCCCCAATCTCCCAGATGCTGATTCAGCCAG-3′
180°
Prom-L 5′-GGGATTAATATGATTAAGACCCTCTAACCCCCACAAGTTGCTGATTCAGCCAG-3′
fold change vs hGnat1_hRho
hRHOp
Prom-L
e
Human -GGGATTAATATGATTATGAACACCCCCAATCTCCCAGATGCTGATTCAGCCAG-
Pig -GGGATTAATATGATTAATAACGCCCCCAATCTCCCAGGTGCTGATTCAGCCCA-
Pika -GGGATTAATATGATTATGATAACCCCCAAACTCCCCCGGTGCTGATTCAGCCGA-
Alpaca -GGGATTAATATGATTAATAATGCCCCCAATCGCCCAGGTGCTGATTCAGCCAG-
Dolphin -AGGATTAATATGATTAATAACGCCCCCAATCTCGCAGGTGCTGATTCAGCCAG-
Cat -GGGATTAGTATGATTAATAATGCCCCCAATCTTCCAGGTGCTGATTCAGCCAG-
Opossum -GGGATTATTATGATTAGTCATGCCCTGAATCTTCTGGGTGCTGACACTAGGGA-
Wallaby -TGGATTATTATGATTAATTATGCCCTGAATCTTCTGGGTGCTGACTCCATAGA-
Platypus -TGGATTATTATGATTAATAATGCCCCCGATCCCCTGTTTGCTGACCCAGCCGA-
Mouse -GCAGCAGTGGGATTAGCGTTAGTATGATATCTCGCGGATGCTGAATCAGCCT-
f
fold change vs hGnat1_hRho
hRHOp
mRHOp-hRRU
hRHOp-mRRU
mRHOp
mRhop-hRRU -GGGATTAATATGATTATGAACACCCCCAATCTCCCAGATGCTCATTCAGCCTC-
hRhop-mRRU -GCAGCAGTGGGATTAGCGTTAGTATGATATCTCGCGGATGCTGAATCAGCCAG-
g
Relative expression
hRHOp
+ZF5
+KLF15
Prom-L
+ZF5
+KLF15
hRHOp 5′-GGGATTAATATGATTATGAACACCCCCAATCTCCCAGATGCTGATTCAGCCAG- 3′
3′-CCCTAATTATACTAATACTTGTGGGGGTTAGAGGGTCTACGACTAAGTCGGTC- 5′
Prom-L 5′-GGGATTAATATGATTAAGACCCTCTAACCCCCACAAGTTGCTGATTCAGCCAG- 3′
3′-CCCTAATTATACTAATTCTGGGAGATTGGGGGTGTTCAACGACTAAGTCGGTC- 5′